PLASMA FLUCTUATIONS IN AN MPD THRUSTER WITH AND WITHOUT THE APPLICATION OF AN EXTERNAL MAGNETIC FIELD

M. Zuin[?][?] **, V. Antoni**[?][?] **, F. Paganucci*, R. Cavazzana**[?] **, G. Serianni**[?] **, G. Regnoli**[?][?] **, M. Spolaore**[?] **, N. Vianello**[?][?] **, M. Bagatin**[?][?] **, P. Rossetti*, M. Andrenucci***

[?] Consorzio RFX, Associazione Euratom-Enea sulla Fusione
Corso Stati Uniti, 4, I-35127 Padova (Italy)
[?] INFM, Unità di Padova, sez.A, (Italy)
*Centrospazio, Via A. Gherardesca 5, 56014 Pisa (Italy)

ABSTRACT

Reduction of Magneto-Plasma-Dynamic (MPD) thrusters efficiency is observed in critical regimes, characterized by high levels of electric fluctuations. Plasma fluctuations in the plume of a hybrid plasma thruster have been investigated in a range of externally applied magnetic field. The spatial and temporal properties of floating potential fluctuations have also been studied using a matrix of probes. The investigation has shown a strong dependence of plasma fluctuations on the external magnetic field. Magnetic measurements have revealed an electromagnetic nature of these plasma fluctuations. The results suggest an interpretation in terms of magnetoacustic instabilities.

INTRODUCTION

Magneto-Plasma-Dynamic (MPD) thrusters are currently under investigation as they constitute a possible, high power electric propulsion option for primary space mission, ranging from orbit raising to interplanetary mission of large spacecraft.

Presently, one of the major problems facing MPD thruster operation is the onset of critical state found as the power is increased beyond the full ionisation condition. In this regime, large fluctuations in the arc voltage signals and damages to the anode are observed along with performance degradation [1].

To assess these phenomena, an investigation of local plasma parameters by using electrostatic and magnetic probes has been carried out on a MPD thruster, called Hybrid Plasma Thruster (HPT), illustrated in Fig. 1 [1, 2, 3]. The HPT is an axisymmetric MPD thruster with an applied magnetic field, a central acceleration
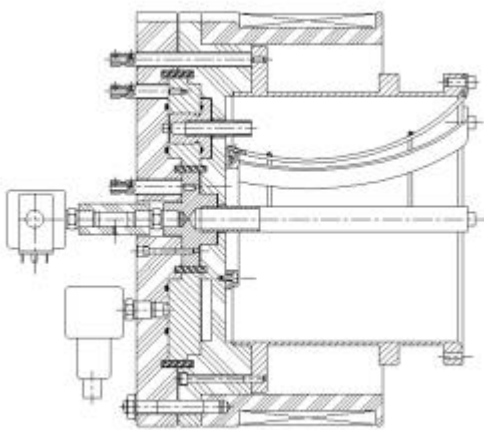

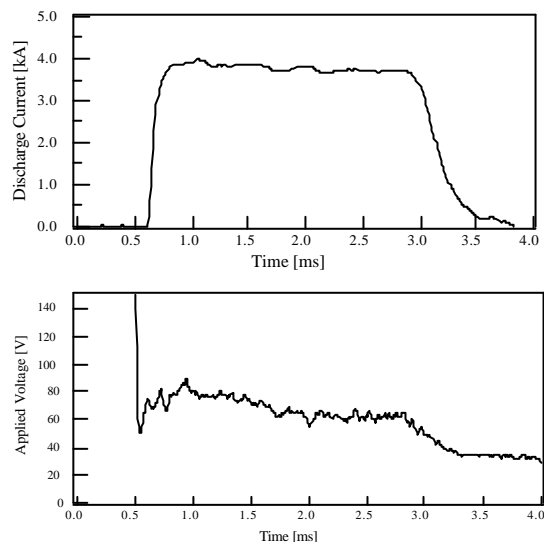Fig. 1: The Hybrid Plasma Thruster (HPT)

Fig. 2: Typical arc current and voltage signals

chamber and a peripheral ionization chamber. The resulting magnetic field is a combination of that self-generated by the flowing current and that produced by external coils. The thruster has a central 20 mm in dia hollow cathode, an anode, consisting of a cylinder 200 mm in dia and eight straps, which divide the central chamber from the ionization chamber, eight peripheral hollow cathodes 12 mm in dia and a solenoid, capable of producing an induction field up to 100 mT at the thruster axis. The aim of the peripheral chamber is the ionization of a small fraction of the propellant by means of a secondary, low power, discharge between the

peripheral cathodes and the anode. The ionized propellant then flows in the acceleration chamber, increasing plasma density near the anode.

The thruster has been operated in a pulsed, quasi-steady mode (pulse length of 2.5 ms, Fig. 2), with argon as propellant (660 mg/s), with and without the application of the external magnetic field (B max on the axis up to 80 mT), for instantaneous power inputs ranging from 150 to 1000 kW. On the thruster under examination it is generally found that the improvement due to the applied magnetic field is considerably large only at low current regimes. The analysis has been focused on the effect of this externally applied field on the thrust and in particular at high current where a degradation of the performance is normally observed [1].

Magnetoplasmadynamic instabilities have been proposed to favour the 'onset' phenomenon, limiting the development of highly efficient plasma accelerators.

In order to understand the role of plasma fluctuations in the deterioration of the overall performance an investigation of the mean and fluctuating magnetic field and plasma parameters such as electron density and temperature, and floating potential has been performed.

DIAGNOSTIC DESCRIPTION

Two systems of electric probes and one system of magnetic probes have been developed. The first system of electric probes, named 'Rake' probe, consists of 7 aligned graphite electrodes, 8 mm apart from each other, and housed in a boron-nitride case. The system was placed at 80 mm from the thruster outlet, with the deepest inserted probe on the thruster axis. The probes have been used in a five-pin balanced triple probe configuration [4] to obtain simultaneous measurements of plasma potential, electron density and temperature. The second system of electric probes consists of two concentric rings of respectively 60 and 100 mm radius, each housing 32 equally spaced electrodes. The system was placed coaxially to the thruster axis, at 80 mm from the thruster outlet. The 2D space and time correlations of floating potential fluctuations in the plume have been investigated.

The magnetic probe system consists of two probes housed in a quartz tube and spaced by 15 mm, each probe measuring the three magnetic field components in the same location.

All data have been collected by connecting the probes to a digital oscilloscope (Yokogawa DL716) with 12 bit resolution and isolated inputs, at a sampling frequency of 10 MHz. The estimated analog signal bandwidth was 500 kHz for electric, and 1MHz for magnetic probe signals.

A more exaustive and complete description of all the diagnostic instruments used in this experimental campaign can be found in [5].

PLASMA CHARACTERIZATION

The mean values of electron temperature and density in the plume of the thruster have been measured at a fixed distance of 80 mm from the thruster outlet, in different radial positions and operating conditions. A current range between 4.3 and 8.2 kA has been investigated.
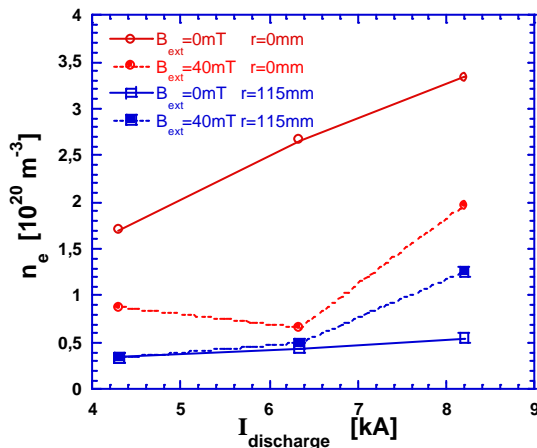

Fig. 3: Density at different currents for two radial positions, with and without external magnetic field.
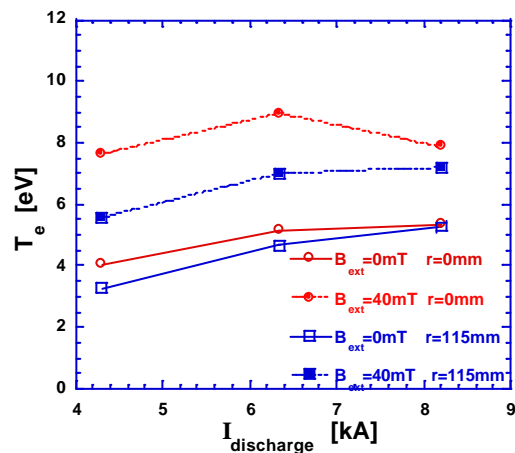
Fig. 4: Electron temperature values at different currents for two radial positions, with and without external magnetic field.

Density is typically of the order of some 10^{20} particle/m^3, peaked around the axis (r = 0 mm), as shown in Fig. 3. By increasing the input power, the difference between the value on axis and off-axis (r = 115 mm) slightly increases, indicating a tendency to peaking with increasing current.

The application of the external magnetic field B_{ext} reduces the electron density on axis and increases that at r = 115 mm, flattening the profile, and this flattening tendency is more pronounced at higher currents. T_e values in the same experimental conditions are shown in Fig. 4. They span from 3 to 5 eV without the external magnetic field, from 6 to 9 eV when this is applied. Electron temperature shows a slight tendency to increase with current, while its radial profile results rather flat. To summarize, it has been observed that without B_{ext} density profiles are peaked while temperature profiles are flat. The application of B_{ext} increases the temperature and reduces the density, flattening its profile. Therefore the fact that the thrust is strongly affected by the application of the external magnetic field indicates some relationship between profiles of density and temperature and thruster performance. In a wide category of magnetized plasmas, including those studied for thermonuclear fusion experiments, it's known that plasma fluctuations regulate plasma profiles. This analogy has motivated the fluctuations investigation described below.

PLASMA FLUCTUATIONS

The electrostatic fluctuations have been studied in order to characterize the regimes with and without external field focusing in particular on the onset of the critical regimes at high power.

In Fig. 5 the Root Mean Square (RMS) of density fluctuations, normalized to the density mean value,
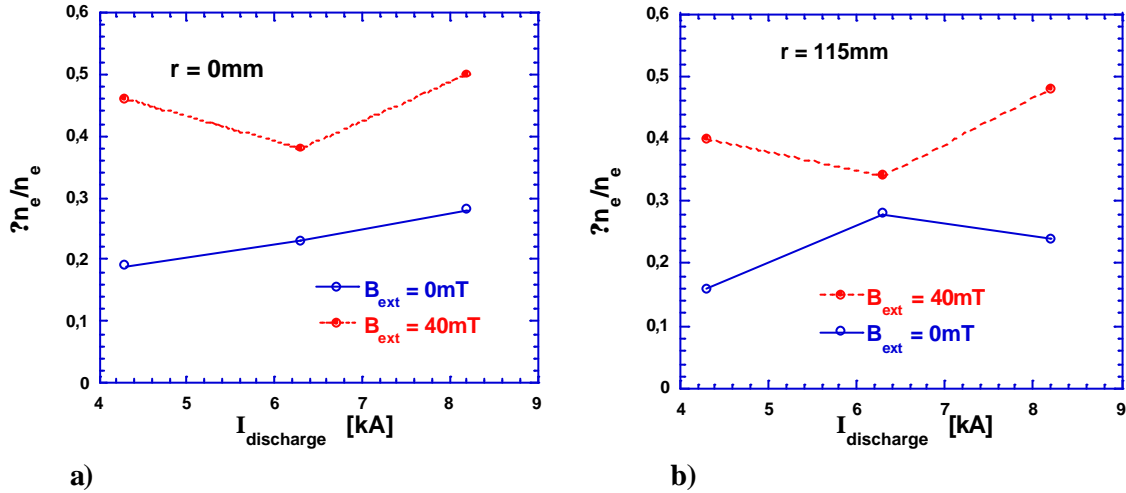
a)   b)

Fig. 5: Average RMS value of n_e normalized to average n_e value as a function of current for two different radial positions: r = 0mm [a] and r = 115 mm [b], both with and without B_{ext}.
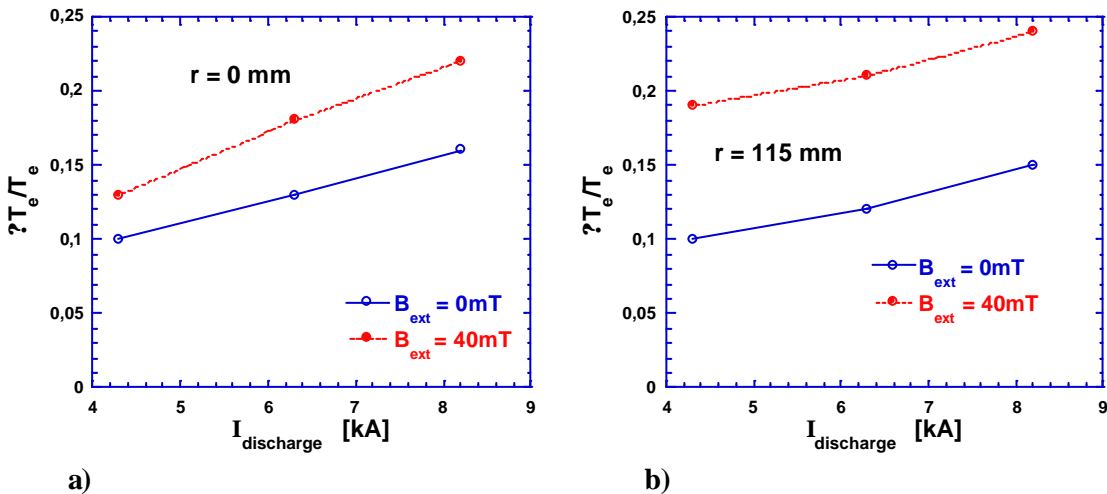
a)   b)

Fig. 6: Average RMS value of T_e normalized to average T_e value as a function of current for two different radial positions: r = 0mm [a] and r = 115 mm [b], both with and without B_{ext}.

obtained by averaging over 1 ms during the discharge, are shown, for two different radial positions.

Typical values without magnetic field are of the order of 20%, while the application of an external magnetic field causes a doubling of the RMS level. No clear dependence on radial position and/or applied power has been observed. In Fig. 6 are shown for the same positions the normalized temperature fluctuations RMS. Their values are typically half the values for density fluctuations, while their behaviour with applied B_{ext} is similar. A slight tendency to increase with current can be observed.

In Fig. 7 RMS values for floating potential fluctuations are plotted as a function of current for four different values of the applied external magnetic field. Their absolute values increase with the current and external magnetic field. For the experimental conditions in which temperature has been investigated (B_{ext}=0 and 40 mT), the RMS values have been normalized to the mean temperature, showing similar behaviour as discussed below.

In general it's observed that all plasma fluctuations increase with the external magnetic field. Floating potential fluctuations exhibit the most pronounced dependence on magnetic field, and therefore the analysis has been focused on their properties to find out the relationship with the critical regimes, mentioned above, appearing at the highest current.

Fig. 7: Average RMS value of floating potential (evaluated at r=6 cm) as a function of current for different values of the external magnetic field.

To obtain insight on the origin and time behaviour of these fluctuations a spectral analysis of the fluctuating quantities has been performed. This analysis has been focused on the floating potential collected by the annular system of probes located at r = 60 mm, in order to achieve information in space and time correlations properties.

In normal condition, without external applied magnetic field, the power spectra of the signals show a peak (as shown in Fig. 8 a)), whose frequency increases almost linearly with the current from about 40 kHz at $I_{discharge}$=4.2 kA up to 70 kHz at 8.2 kA. The application of B_{ext} causes a slight increase of the dominant frequency up to 90 kHz at 8.2 kA. To highlight the dependences of the frequency peak, in Fig. 8 b) this is shown, as a function of current, without magnetic field and for three different external magnetic fields. An almost linear dependence on current is observed, while the external magnetic field seems to have slight influence.
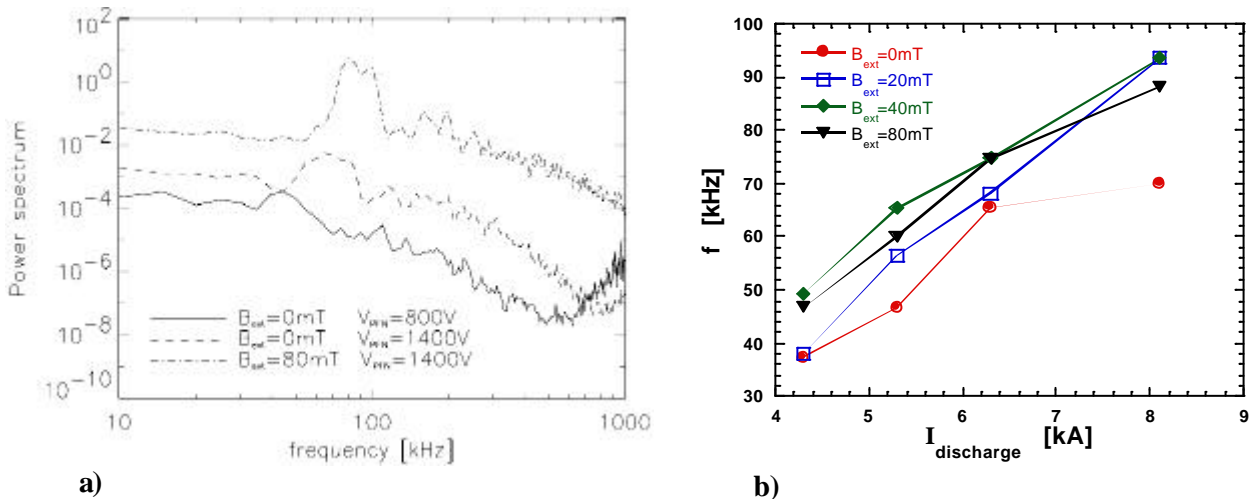

a)

b)

Fig. 8: a) Power spectrum of floating potential signals in three different conditions of external magnetic field and applied voltage, b) dependence of dominant frequency on current and external magnetic field.

The signals correlation has been studied by Fourier decomposition in the azimuthal direction. The results of the mode dynamics analysis are shown in Fig. 9 in three different conditions. At low current, in absence of B_{ext}, only a global m=0 mode is revealed, while the application of the external magnetic field causes the

4

appearance of an azimuthal m=1 mode, with wavelength $\lambda \simeq$ 37.7 cm, at r = 6 cm. It is worth noticing that a similar m = 1 mode appears at the highest current (8.2 kA) also without B_{ext}.
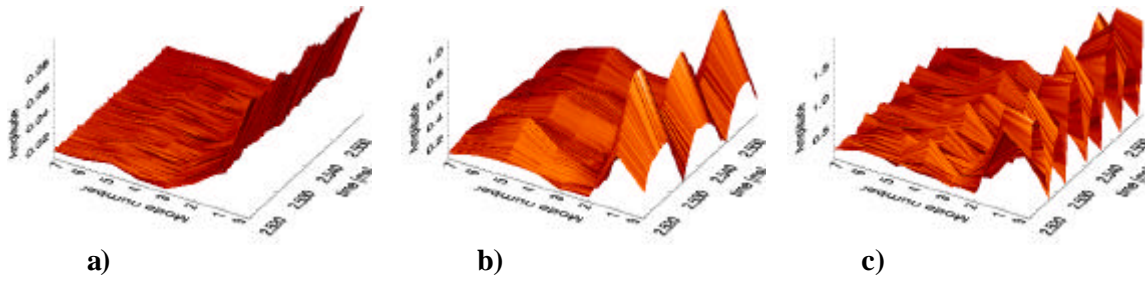

a)   **b)**   **c)**

FIG. 9: Mode amplitude time evolution of floating potential of the probes located at r= 60 mm with: a) B_{ext}=0 mT, $I_{discharge}$=4 kA; b) B_{ext}=40 mT, $I_{discharge}$=4 kA; c) B_{ext}=40 mT, $I_{discharge}$=6 kA.

Modes of higher order are observed sometimes to compete with the dominant m = 1 mode, at a frequency of the same order and with the same current dependence of that of the dominant mode. As a consequence the frequency peak results mainly assigned to the dominant m=1 mode. Similar results have been obtained by the analysis of data collected on the array at r =10 cm.
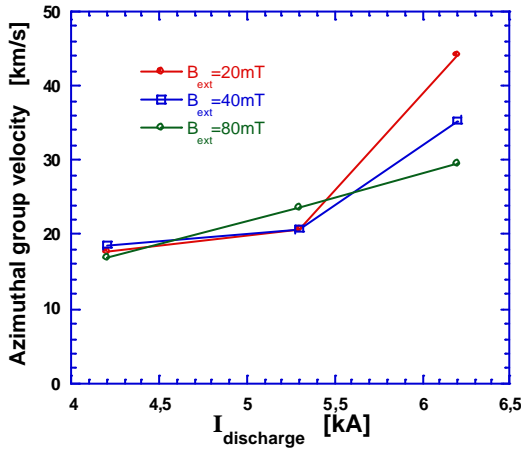

Fig. 10: Group velocity as a function of current, for different values of B_{ext}.

The phase velocity can be calculated as $v_{ph}=\omega/k$, where k=m/r, and $\omega=2\pi f$. As observed for the frequency, the phase velocity is no strongly dependent on the applied magnetic field and it spans in the range between 10 and 35 km/s (evaluated at r=6 cm). Also a group velocity has been derived from the time required for a complete turn of a defined potential peak. As seen in Fig. 10 this velocity increases with current, and for $I_{discharge}$=6.2 kA decreases with the applied magnetic field. These results, combined with the fact that without external magnetic field no group velocity can be identified, suggest that this rotation is due to electric (ExB) or pressure-gradient (Bx∇P) drift effects.

POWER LOSSES AND FLUCTUATIONS

The observed relationship between plasma fluctuations and the critical regimes fosters the investigation of the effect of these fluctuations on thruster efficiency. The thruster efficiency is defined as the ratio of the thrust power upon the total power. The thrust power can be evaluated as $W_{prop}=T^2/(2\dot{m}\,I)$, where $\dot{m}$ is the mass flow rate, T is the thrust, and I is the current passing throw the electrodes. The thrust value was obtained by ballistic method, which measures the impulse of the thrust for each shot, and was computed by dividing the measured impulse by the pulse duration for each shot. Therefore the power lost can be obtained by subtracting the thrust power to the total power, and it results almost 80% of the latter one. The losses are due to different processes, some of which are known, and can be quantified as those due to cathode and anode falls, and ionization processes [6]. However these processes account only for 10% of the losses. The mechanism underlying the remaining major lost power, hereinafter referred as 'Lost Power', is matter of debate, which the present fluctuations study is aimed to contribute to.
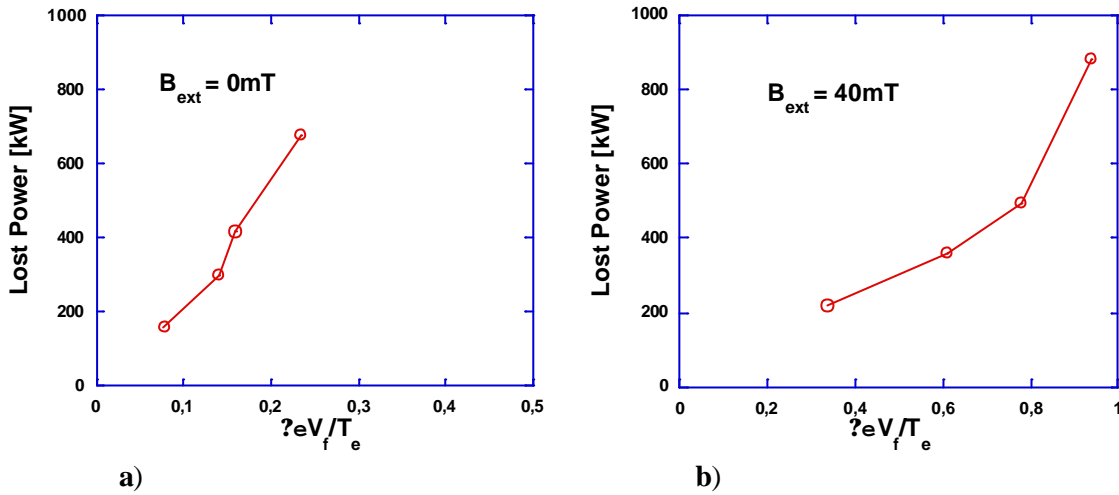
Fig. 11: Lost Power vs fluctuation levels of floating potential (normalized to the electron mean temperature) without [a] and with [b] an applied external magnetic field of 40 mT.

In Fig. 11 this Lost Power is shown as a function of the floating potential RMS, normalized to the mean temperature. It results that the lost power increases with increasing fluctuation levels, both with and without the applied external magnetic field. This result proves that plasma fluctuations are related to power losses and therefore are candidate to trigger the onset of critical regimes.

DISCUSSION ON THE ORIGIN OF THE ELECTROSTATIC FLUCTUATIONS

In order to obtain some insight on the origin of these fluctuations, a key information is the identification of their nature. Some authors [7, 8, 9, 10] have devoted their attention to study the instabilities that could grow in an electromagnetically accelerated plasma. In some paper the problem of current-driven microinstabilities that should degrade the efficiency of an MPD accelerator was considered. In some experiment [7] it has been found that the dominant unstable mode falls near the lower hybrid frequency.

In the plasma under our investigation lower hybrid frequency is about 5 MHz, and so is much higher than the frequency range in which power spectra show their peaks.

It must be noted that lower hybrid frequency (f_{lh}) is a resonance frequency that belongs to the class of instabilities known as 'magnetoacustic' (or magnetosonic) waves. At frequency much lower than the hybrid one, magnetoacustic waves should have a phase velocity equal to the Alfvén velocity ($v_A = B/(?_0?)^{1/2}$, where ? is the mass density of the used gas). In Fig. 12 the azimuthal component of the phase velocity of the dominant mode and the Alfvén velocity calculated in a case with applied external magnetic field are shown. The phase velocity of the dominant mode is very close to the Alfvén velocity, and it grows almost linearly with the current (i.e. the self generated magnetic field), suggesting a magnetoacustic origin of the mode.
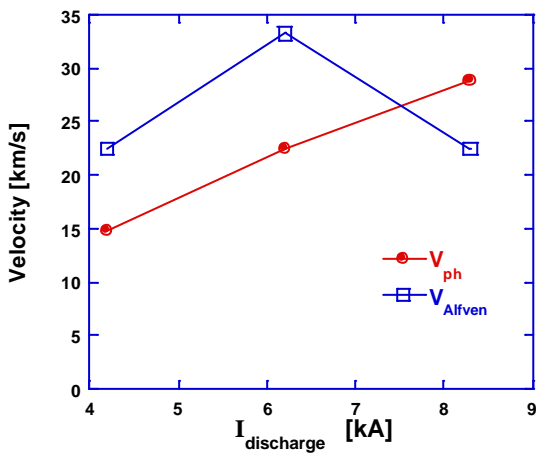

Fig. 12: Alfvén velocity calculated for $B_{ext}=40$ mT and phase velocity of the dominant m=1 mode in the same condition, as functions of current.

It is worth to note that these waves cannot be interpreted as pure shear Alfvén waves as found in similar experimental apparatus [10], because shear Alfvén waves have a resonance at the ion cyclotron frequency, rather below the observed peaks (? $_i$?15?20 kHz).

The magnetosonic wave is an extraordinary wave, because its electric field is oriented everywhere perpendicular to B, giving rise to 'extraordinary' phenomena due to Lorenz force. Unlike the shear or torsional Alfvén wave the magnetosonic wave 'compresses' the plasma, and is sometimes referred to as 'compressional Alfvén wave'. The wave can propagate across the magnetic field, alternately compressing and expanding it like the pressure in a sound wave, thus the name 'magnetoacustic'.

6

MAGNETIC FLUCTUATIONS

The magnetoacustic origin proposed for these fluctuations has motivated the study of the magnetic fluctuations. In particular the fluctuations of the self-generated magnetic field have been measured in the inner region of the thruster, close to the cathode. The two magnetic probes were aligned along the axial direction, and located 6 cm radially apart from the axis and at 7 cm from the cathode tip along the thruster axis.

Very large amplitude fluctuations have been found. In Fig. 13 the RMS value of the azimuthal component of the magnetic field, normalized to the mean value, is shown. Magnetic fluctuations increase with current, up to 35% of the mean magnetic field. In the same figure the normalized floating potential RMS are also reported for comparison. Both fluctuations exhibit the same trend with the current. Focusing on the magnetic field components in the plane perpendicular to the direction of the dominant azimuthal field (namely along r and z), the fluctuations power spectra exhibit peaks in the same range of frequencies as reported for the electrostatic spectra.
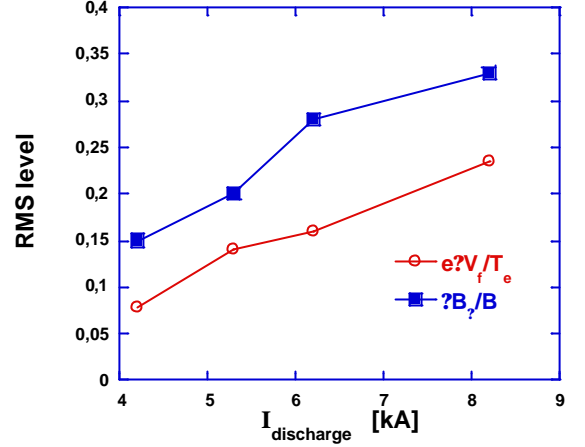

Fig. 13: Comparison between magnetic fluctuation levels (normalised to mean values) and floating potential levels (normalised to mean electron temperature) as functions of current
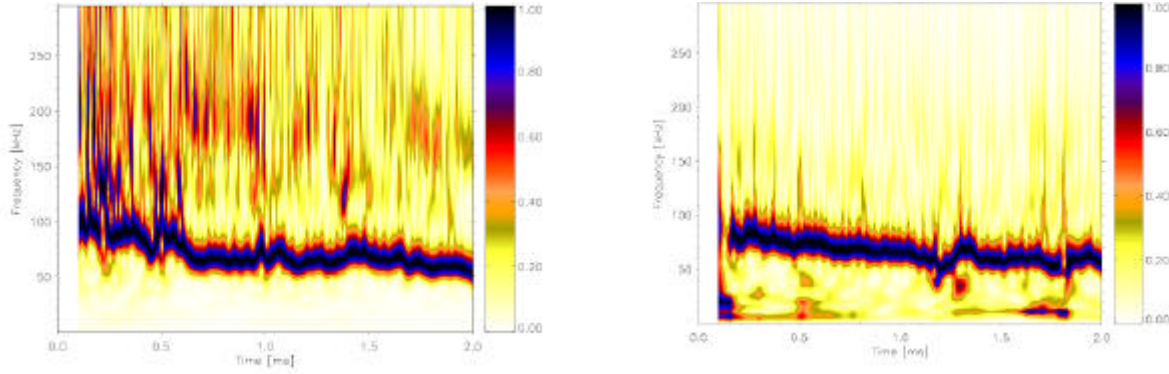
In Fig. 14 the wavelet spectra show the time evolution of the dominant mode, both for magnetic (radial direction) and electrostatic fluctuations, confirming that also temporal evolution is similar. Therefore spectra and RMS behaviours confirm the electromagnetic nature of the instabilities behind the plasma fluctuations.

Phase analysis between the signals of radial and axial magnetic fields has shown an almost constant phase difference of $+\pi/2$. This means circular (right) polarization of the fluctuations in the plane r-z, further in favour of the hypothesis of magnetoacustic wave discussed above.

a)   b)

Fig. 14: Comparison between wavelet fluctuations spectra for magnetic (along radial directions) [a], and floating potential signals [b].

MAGNETIC FLUCTUATIONS PROPAGATION

In this Section the results of the reconstruction of the spectral density $S(k_z,f)$ are presented, where k_z is the wavenumber in the axial direction and f is the frequency. The reconstruction was performed on a statistical basis, using the measurements of the two magnetic probes aligned in the z direction. The numerical technique [11, 12] proceeds as follows: the signals y_1 and y_2 of the two probes are divided into N slices of equal length, $y_1^{(i)}$ and $y_2^{(i)}$ (i = 1...N). The slices are considered as independent realizations of the stochastic process under study. For each slice, the discrete Fourier transforms $\tilde{y}_1^{(i)}(f)$ and $\tilde{y}_2^{(i)}(f)$ are computed. From these, the power $S^{(i)}(f) = (|\tilde{y}_1^{(i)}(f)|^2 + |\tilde{y}_2^{(i)}(f)|^2)/2$ and the cross-phase $\phi^{(i)}(f) = \arg\{[\tilde{y}_1^{(i)}(f)]^*\tilde{y}_2^{(i)}(f)\}$ are computed. The cross-phase is used to obtain an estimate of the wavenumber in the direction connecting the two probes, $k^{(i)}(f) = \phi^{(i)}(f)/\Delta x$, where Δx is the distance between the probes. These results are used to

progressively fill a histogram of the spectral density, i.e. for each frequency f the bin corresponding to the wavenumber $k^{(i)}(f)$ is increased by the amount $S^{(i)}(f)$. By repeating this procedure for all slices, the resulting histogram of S(k,f) is a statistical estimate of the true spectral density function. In this analysis the stationarity of the process under study, and ? x much smaller than the fluctuation wavelength are assumed.

The $S(k_z,f)$ computed as described above, for the probes measuring the radial component of the fluctuating magnetic field is shown in Fig. 15, for two different experimental conditions. Each frame has a different colorscale, in order to make each plot most readable. The most important features of these plots are the presence of some kind of continuum in the magnetic fluctuations up to 400 kHz. At high power also a relatively sharp peak appears in the spectral density, corresponding to a coherent mode, at frequencies around 70 kHz. The peak and the continuum are found to lie along a line passing through the origin, indicating a dispersion relation ? ~ $k_z v_{ph}$, where v_{ph} is the phase velocity of the waves.

In the same frames lines ? = $k_z v_A$ are also shown (straight lines). The different colors refer to different possible propagation angles, between the wave direction and the z-direction. In calculating v_A the experimental mean magnetic field values, measured by the magnetic probes, have been used.

In the plasma under consideration the electrons are considered to be magnetized (electron cyclotron period much shorter than time-scales of interest), while the ions are not completely magnetized (mean free path for collisions shorter than the Larmor radius, and ion cyclotron period comparable with the other time-scales). In this case Hall effect can introduce strong variations in the dynamics of the system. In such a case the Hall term must be retained in Ohm's law, and the Hall-MHD model must be used. In the approximations of low ? plasmas (where ? is the ratio between the particle pressure and the magnetic pressure, $? = p/(B^2/2?_o)$), the dispersion relation for magnetoacustic wave, in its simplest form, becomes [13]:

$$? ^2 ? \frac{v_A^2 k^2}{2}(1 ? (1 ? ?^2)\cos^2 ? ? [1 ? 2(1 ? ?^2)\cos^2 ? ? (1 ? ?^2)^2 \cos^4 ?]^{1/2})$$

where ? is a dimensionless wavenumber $? = ?/?_i$, $?_i$ is the ion cyclotron frequency, and ? is the angle between the mean magnetic field and the direction of propagation of the wave.

This reduces to the MHD version of the wave if $? << ?_i$.
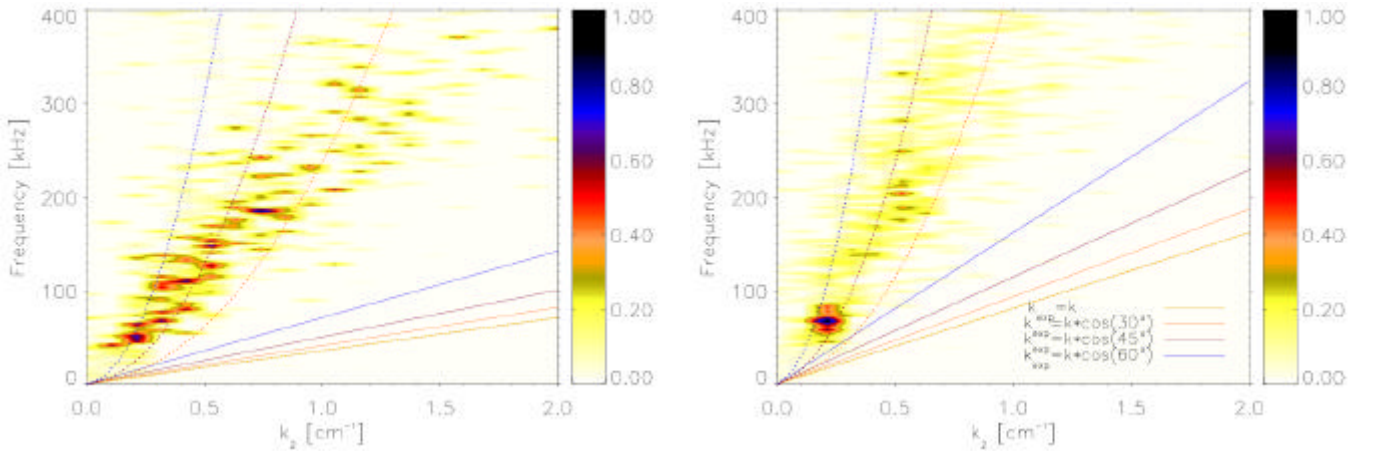
        a)   b)

Fig. 15: Comparison between experimental dispersion relation of the magnetic fluctuations and magnetosonic wave equation, with (dashed lines) and without (straight lines) Hall corrections, for $I_{discharge}$= 5.2 kA a), and 8.2 kA b).

This dispersion relation is also reported in Fig. 15 (dashed lines), taking into account the different possible propagation angles. A more detailed analysis should include non-linear evolution of the waves and the coupling between the shear Alfvén and magnetosonic waves due to ? finite effects and plasma non-uniformities. It must be said that no Doppler shift corrections due to the plasma motion has been applied to the measured frequencies. This effect would force the experimental phase velocities to lower values, and the correction could introduce at most a factor 2. Nevertheless even in this simple form the agreement between theory and experiment seems to confirm a possible 'Alfvénic' nature of the instabilities.

CONCLUSIONS

A study of the fluctuations of electron density, temperature, floating potential and magnetic field in an MPD thruster with and without externally applied magnetic field has been performed.

The normalised RMS of density result larger than those for temperature and the application of an external magnetic fie ld increases all fluctuation levels. RMS values of floating potential signals increase almost linearly with power, indicating that the thrust degradation has some relationship with plasma instabilities. A pulsing m=1 mode in the azimuthal direction appears as the power is increased and with the application of the external magnetic field. The frequency associated to this mode increases almost linearly with current, and its related phase velocity results very close to the Alfvén velocity. Analysis of magnetic fluctuations shows similar dominant frequencies in their power spectra, with circular right polarization in the plane perpendicular to the direction of the main azimuthal magnetic field. Experimental wavenumbers in the axial direction imply dispersion relations that well agree with the hypothesis of an Alfvénic nature of these instabilities.

REFERENCE

[1] F. Paganucci et al., *Performance of an Applied Field MPD Thruster*, IEPC-01-132, 27th International Electric Propulsion Conference, October 14-19, 2001, Pasadena, CA.

[2] V.B. Tikhonov et al., *Investigation on a New Type of MPD Thruster*, OR 21, 27th European Physical Society Conference on Controlled Fusion and Plasma Physics, 12-16 June 2000, Budapest, Hungary, 12-16 June 2000.

[3] V.B. Tikhonov et al., *Development and Testing of a New Type of MPD Thruster*, IEPC-01-123, 27th International Electric Propulsion Conference, October 14-19, 2001, Pasadena, CA.

[4] H. Y. Tsui et al., Rev. Sci. Instrum. **63**, 4608 (1992).

[5] M. Andrenucci et al., *Diagnostics of an Applied Field MPD Thruster*, 28th International Electric Propulsion Conference, March 17-21, Toulouse, France.

[6] M. Andrenucci, F. Paganucci, *MPD Thruster Plume Diagnostic*, IEPC-93-141, 23rd International Electric Propulsion Conference, September 13-16, 2001, Seattle, WA.

[7] D. L. Tilley, E. Y. Choueiri, A. J. Kelly, and R. G. Jahn. *Journal of Propulsion and Power,* 12(2):381--389, 1996.

[8] H. P. Wagner, H. J. Kaeppeler, M Auweter-Kurtz. *Journal-of-Physics-D-Applied-Physics*. March 1998; 31(5): 529-41.

[9] H. P. Wagner, H. J. Kaeppeler, M Auweter-Kurtz. *Journal-of-Physics-D-Applied-Physics*. March 1998; 31(5): 519-28.

[10] R. Hatakeyama, M. Inutake, T. Akitsu, Phys. Rev Lett. 47, n.3 (1981).

[11] J. M. Beall, Y. C. Kim, and E. J. Powers, J. Appl. Phys. **53**, 3933 (1982).

[12] S. J. Levinson, J. M. Beall, E. J. Powers, and R. D. Bengston, Nucl. Fusion **24**, 527 (1984).

[13] N.F. Cramer, *The Physics of Alfvén Waves*, ed. Wiley-VCH (2001).